JOURNAL OF APPLIED ELECTROCHEMISTRY 12 (1982) 153–162

Anodic formation of thin CdS films. I. Kinetics and mechanisms under galvanostatic and potentiodynamic conditions

L-S. R. YEH, P. G. HUDSON, A. DAMJANOVIC

Corporate Research & Development, Allied Corporation, Morristown, New Jersey 07960, USA

Received 21 May 1981

The formation of thin anodic films of CdS is studied in 1 mol dm^{-3} $NaHCO_3$ + 0.1 mol dm^{-3} Na_2S solutions under galvanostatic and potentiodynamic conditions. Under both experimental conditions, films up to about 50 Å are formed according to the high field model of growth. In this thickness range an insufficient space charge is developed to noticeably affect the kinetics. From galvanostatic experiments at different temperatures, the activation energy was determined to be 10.6 kcal $mole^{-1}$. The surface density, N, of the species participating in the rate determining step is unusually low, about 5×10^6 cm^{-2}. So low a value for N precludes a process at the Cd/CdS interface as the rate determining step. The significance of various parameters in the observed rate equation are compared with and discussed in relation to the respective parameters in the rate equations developed for the high field model of growth.

1. Introduction

Electrochemical formation of thin photoconductor films has received increasing attention in the last few years. This was triggered by the demonstration of Miller and Heller [1] showing that polycrystalline CdS films formed anodically on a cadmium surface in 1 N NaOH in the presence of Na_2S can replace single crystal CdS and can, under photoexcitation, drive a sulphide–polysulphide liquid junction solar cell. In another demonstration, Hodes *et al.* [2] showed that cathodically codeposited Cd and Se on a conducting substrate might offer, after subsequent thermal treatment, a viable alternative for photoconductor formation and could be used in a liquid junction solar cell.

Among possible candidates for the electrochemically formed photoconductors to be used in solar cells is thin film CdS grown anodically on Cd substrates although its band gap (2.4 eV) is rather high. Efficiencies of liquid junction cells using electrochemically formed CdS are substantially lower than the efficiencies of the cells with single crystal CdS under comparable conditions [3, 4]. The low efficiencies were attributed to the high density of the recombination centres either at the surfaces of or within the crystallites [3].

Miller *et al.* [4] and Peter [5] studied in detail the formation of the CdS films and processes that occur at the Cd/solution and CdS/solution interfaces. The formation of CdS resembles the anodic passivation of metals and growth of oxide or hydroxide barrier layers. Following the initial adsorption and buildup of a passivating layer of monomolecular dimensions, a film about 50 Å thick grows in the potential region from about − 1.2 V to about + 0.1 V versus SCE (in 0.1 mol dm^{-3} Na_2S + 1.0 mol dm^{-3} $NaHCO_3$ solutions) by processes that are sensitive to the potential difference across the film, or the inner Helmholtz layer, and the thickness of the film itself. Films appear to be compact and uniformly thick. As these films grow to a thickness of about 50 Å and the electrode exceeds a critical potential, i.e. in constant current or potential sweep experiments, the kinetics abruptly change [4, 5]. Growth then proceeds more rapidly and the film thickens to 5000 Å, or more, presumably by a diffusion controlled process [5]. These thick films are apparently less compact [5]. It is not clear why the growth kinetics and mechanism change abruptly

0021–891X/82/020153–10$03.00/0 © 1982 Chapman and Hall Ltd.

at about 50 Å and films of apparently inferior quality grow.

Kinetics and mechanism of growth when the films thicken from monomolecular dimensions to about 50 Å have recently been studied in some detail [4, 5]. Growth at a constant current appears to be well accounted for in terms of the Cabrera–Mott model of the high field assisted formation of insulating films. Significantly, however, according to Peter [5], the growth kinetics at an applied constant potential are described, not by the inverse logarithmic law as would be required by the Cabrera–Mott model, but rather by the so-called direct logarithmic law according to which charge density at a constant potential imposed across the electrode increases with the logarithm of time. Peter [5] attempted to reconcile this difference in terms of the Cabrera–Mott model and the inverse logarithmic law but modified for the change in the potential difference across the inner Helmholtz layer, and hence across the oxide film itself. This attempt, however, did not meet with any success. In the growth of oxide films at Pt electrodes, an equivalent modification brought the galvanostatic and potentiostatic data into full agreement and proved that the same mechanism controlled the growth under both experimental conditions [6, 7]. It would, therefore, appear that different mechanisms may indeed control the formation of the CdS films under galvanostatic and potentiostatic modes of growth.

In this paper, we examine the kinetics of the initial stages of growth of CdS under potentiodynamic conditions at various sweep rates at room temperature as well as under galvanostatic conditions at different temperatures. It was hoped that these experiments would further the knowledge of the kinetics of CdS growth and shed additional light on the mechanisms of growth and possible changes in the mechanisms with experimental conditions.

2. Experimental procedures

Experiments were conducted in an all glass two-compartment cell. The reference electrode compartment was separated from the main working/counter electrode compartment by a stopcock and Luggin capillary. The reference electrode was a saturated calomel electrode. Unless otherwise indicated, potentials are referred to this electrode. A cadmium rod with a stated purity of 99.999% was tightly fitted into a Teflon tube so that only the disc surface served as the electrode. A platinum coil was used as the counter electrode. The main and reference electrode compartment of the cell were jacketed so that the solutions in both compartments could be maintained at a given temperature by thermostated water circulating through the jacket.

A potentiostat (PAR 173) and function generator (PAR 175) were used for galvanostatic and potentiodynamic experiments. Data were recorded on an X/t–Y recorder (Hewlett Packard 7004B) for slow potential scans or low applied currents. For fast changes of potentials a storage oscilloscope was used (Tektronix 7623A).

For each experiment, the electrode was first mechanically polished with alumina paste (1 to 0.3 μm) then chemically polished for 20 s in a mixture of glacial acetic acid and hydrogen peroxide to give a bright mirror finish. The surface roughness factor (RF) of electrodes prepared this way was found by Breitner and Vedder [8] to be about 1.2–1.3. Working solutions (1.0 mol dm^{-2} $NaHCO_3$ + 0.1 mol dm^{-3} Na_2S) were prepared from reagent grade $NaHCO_3$ and Na_2S and conductivity water.

3. Results

3.1. *Potentiodynamic experiments*

In preliminary experiments a linear potential scan from − 1.5 to + 2.0 V was applied to freshly polished electrodes in a 1.0 mol dm^{-3} $NaHCO_3$ solution with and without the addition of 0.1 mol dm^{-3} Na_2S. Voltamograms for these two cases are shown in Fig. 1. In $NaHCO_3$ solutions without Na_2S (pH = 8.2), a large anodic peak, presumably due to the formation of $Cd(OH)_2$ and rapid corrosion, appears at about − 0.7 V. In $NaHCO_3$ solutions with Na_2S (pH = 9), a much smaller anodic peak appears at about − 1.2 V while the peak previously observed at − 0.7 V is entirely suppressed. According to Miller *et al.* [4] and Peter [5], who also observed a peak at about − 1.2 V, the current under this peak represents the discharge of hydrosulphide ions which are then used in the formation of CdS. Integration of the

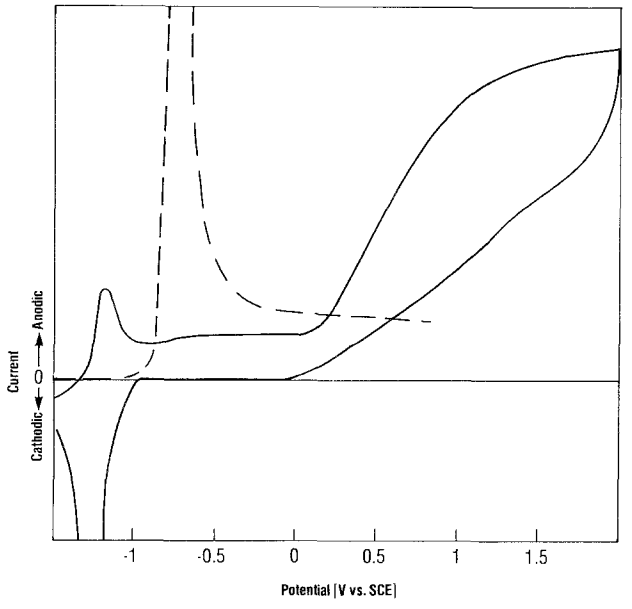

Fig. 1. Cyclic voltamograms of a Cd electrode in 1.0 mol dm^{-3} $NaHCO_3$ + 0.1 mol dm^{-3} Na_2S (solid line, pH 9.0), and in 1.0 mol dm^{-3} $NaHCO_3$ solution (dashed line, pH 8.2). Electrode area is 1.27 cm^2 and scan rate 100 mV s^{-1}.

charge under the peak, about 200 $\mu C\,cm^{-2}$, indicated that a monolayer of CdS was formed.

A characteristic feature of the voltamogram in the presence of Na_2S is a current plateau following the peak at − 1.2 V. The plateau region extends for over 1.0 V. A large increase in anodic current was observed at potentials beyond + 0.1 V. It corresponds to an extended growth of CdS films [4, 5]. When a prereduced electrode is placed into the solution, a small cathodic current is first observed at potentials between − 1.5 and − 1.2 V. This current decays to zero in 1–2 min. In open circuit, a rest potential close to − 1.1 V is established in about 1–2 min. If the potential scan is applied from the rest potential, no peak is observed (of course!) and the plateau region becomes fairly well defined (Fig. 2). In a series of experiments, always with freshly polished electrodes, potential sweeps with different scan rates, S, are applied to the electrodes from the rest potential. As expected, the plateau current density, i_s, increases with S, as shown in Fig. 3. A nearly linear relationship is observed between $\log i_s$ and $\log S$ with a slope close to 1. However, it appears that i_s increases less rapidly with S than required for the linear dependence of i_s on S. A similar deviation from linearity was observed in the studies of anodic growth of $Pt(OH)_2$ and $Ni(OH)_2$ films [9, 10]. It was suggested that a plot of S/i_s against $\log S$ was a more sensitive test for linearity [11]. Such a plot clearly shows that S/i_s for the growth of CdS films is not constant but increases with $\log S$; i.e. i_s is not linearly proportional to S (Fig. 4). Of course, whether i_s is, or is not, linearly proportional to S depends on the mechanism of the formation of CdS in the plateau region as discussed below.

3.2. *Galvanostatic experiments*

In a series of experiments, a constant current was applied to freshly polished Cd electrodes after the electrode had assumed its rest potential in open circuit. A steep, nonlinear rise of potential was observed immediately after the application of a constant anodic current. This initial region of

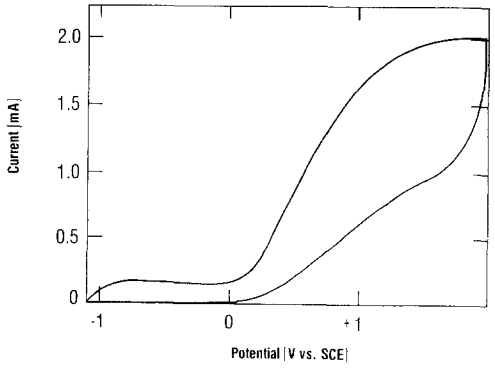

Fig. 2. Cyclic voltamograms of a Cd electrode in 1.0 mol dm^{-3} $NaHCO_3$ + 0.1 mol dm^{-3} Na_2S solution. Scan rate, S, is 100 mV s^{-1}. Potential scan started at rest potential − 1.1 V.

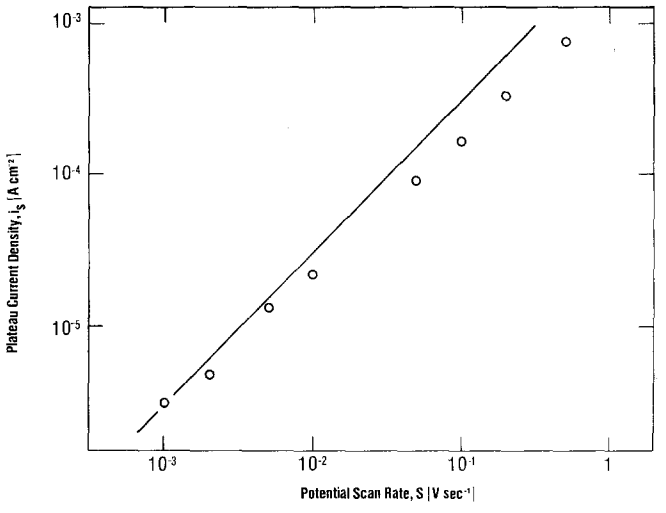

Fig. 3. Variation of plateau current density with potential scan rate. Current densities are not corrected for roughness of the electrode surface. Line drawn through the lower point indicates slope of 1.

growth was followed by a region in which the potential increased fairly linearly with time. Eventually, at still longer times, the potential continued to increase with time but now much more slowly and in a nonlinear fashion (cf. Fig. 5). In Fig. 5, charging curves are shown for 7.9×10^{-4}, 7.9×10^{-5} and 7.9×10^{-6} A cm^{-2} in argon saturated solutions. The time axis is scaled to represent charge density. Evidently, $\partial V/\partial q$ slopes in the linear potential region increase with the applied current density. These slopes are plotted in Fig. 6 against the logarithm of the applied constant current densities for all current densities used in this study. It is evident from Fig. 6 that $\partial V/\partial q$ changes linearly with log i. The linearity extends for at least four decades of current density.

In experiments at different temperatures, similar V–q traces are obtained. However, both the slopes of the linear V–q traces at a given current density and the change of slopes with current density are affected by temperature. This is shown in Fig. 7 with the $\partial V/\partial q$ versus log i dependences at three temperatures.

4. Analysis of the results and discussion

4.1. *Potentiodynamic data*

As shown in a study of growth of anodic films at Pt electrodes [11], if a unique relationship exists between current density for film growth, potential and charge density – or the average thickness of

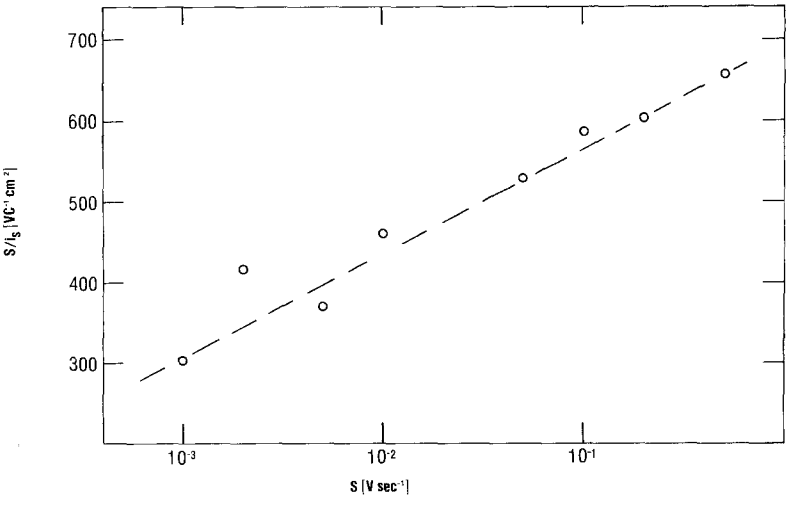

Fig. 4. Ratio of scan rate to plateau current density as a function of scan rate from Fig. 3.

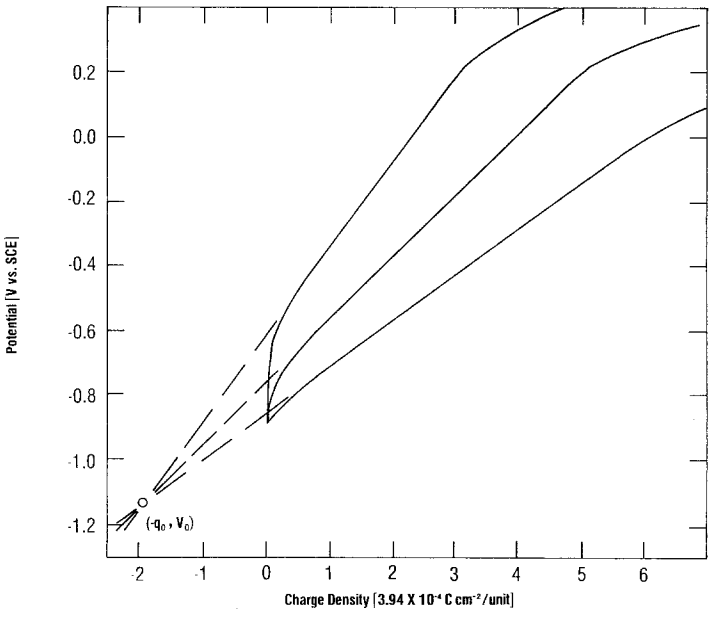

Fig. 5. Galvanostatic charging curves at various current densities. Charge density is 3.94×10^{-4} C cm^{-2} per division. Data are not corrected for roughness of the electrode surface.

the growing film – i.e. if $f(V, i, q) = 0$, then in the plateau region of the voltamograms the following relation holds irrespective of the mechanism by which the film grows

$$\frac{S}{i_s} = \left(\frac{\partial V}{\partial q}\right)_{i_s}. \qquad (1)$$

From Fig. 4, it is evident that $S/i_s \neq$ constant and, therefore, $\partial V/\partial q$ in the plateau region is not independent of S or i_s. $\partial V/\partial q$ increases with S and hence with i_s. The dependence of S/i_s on i_s is shown in Fig. 8. If S/i_s increases linearly with $\log i_s$, as the potentiodynamic data in Fig. 8 indi-

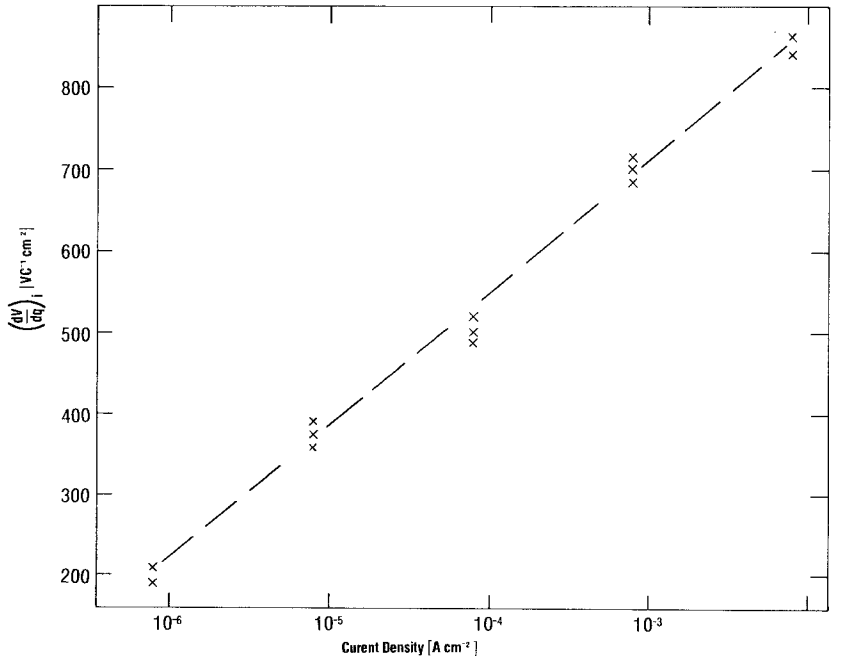

Fig. 6. Slopes of galvanostatic charging curves at various constant current densities. Data are not corrected for roughness of the electrode surface.

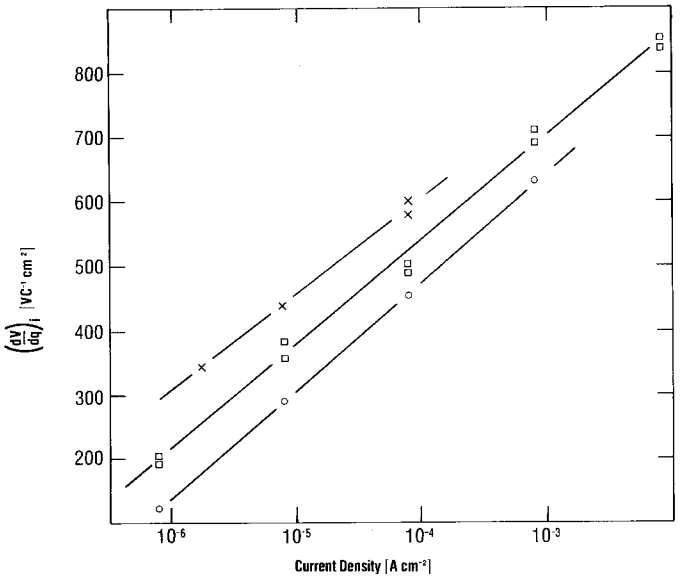

Fig. 7. dV/dq dependence on $\log i$ for 0° C (×), 22° C (□) and 46° C (○). Data are not corrected for the roughness of electrode surface.

cate for at least two decades of current density, then the relationship

$$\frac{\partial V}{\partial q} = \left[\frac{S}{i_s}\right] = a \log \frac{i}{i^0} + b \qquad (2)$$

provides the link between V, q and i. With $i^0 = 1\,\mathrm{A\,cm^{-2}}$, the units of current density are fixed. Constants a and b, corrected for the roughness of the electrode surface (with RF = 1.2), are then equal to 170 and $1300\,\mathrm{V\,C^{-1}\,cm^2}$. This dependence suggests that the known equation for the high field assisted growth

$$i = i_0 \exp\left(\frac{\alpha' \Delta V}{q}\right) \qquad (3)$$

may satisfy the observed potentiodynamic data. If it does, then by comparing Equations 2 and 3, $\alpha' = 2.3\,a^{-1} = 0.014\,\mathrm{V^{-1}\,C\,cm^{-2}}$ and $i_0 = i^0 \exp(-2.3\,b/a) = 1.8 \times 10^{-8}\,\mathrm{A\,cm^{-2}}$. Even if the data in Fig. 8 satisfy the relationship given by Equation 2, a final check of the validity of Equation 3, though possible, would be tedious and prone to various uncertainties and errors [9, 10]. For this reason, potentiodynamic data are not analysed further here, but they will be compared below with the galvanostatic data.

4.2. *Galvanostatic data*

Kinetic data at galvanostatic conditions rep-

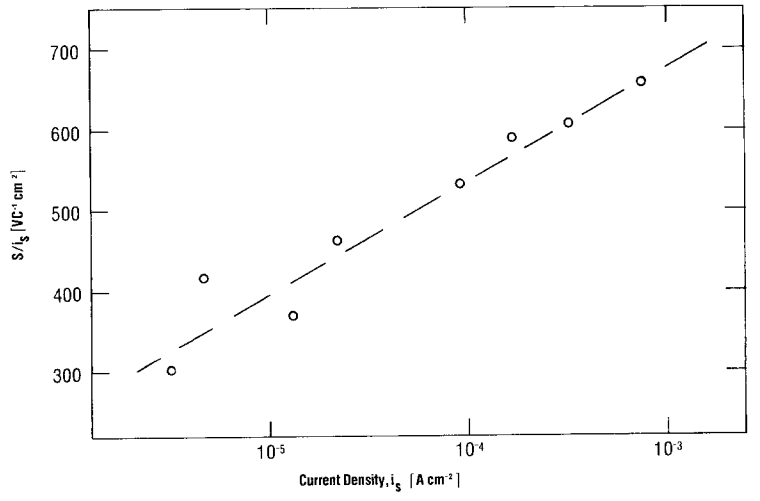

Fig. 8. Ratio of scan rate to plateau current density as a function of plateau current density.

resented by Figs. 5 and 6 lead to the following empirical rate equation

$$i = i_0 \exp\left[\frac{V - V_0}{n(q + q_0)}\right]. \quad (4)$$

Here, q_0 and V_0 are coordinates of the intercept of the extrapolated V–q traces at different current densities (cf. Fig. 5). Experimentally, q_0 and V_0, determined from data like those in Fig. 5, are equal to $650\,\mu C\,cm^{-2}$ and -1.14 V. Parameter n, given by $\partial^2 V/\partial q \partial \ln i$, can be obtained from the slopes of the linear $\partial V/\partial q$ versus $\log i$ lines in Fig. 6. It is equal to $85\,V\,C^{-1}\,cm^2$. The exchange current density, i_0, is related to n and the value of $\partial V/\partial q$ extrapolated to $i = 1\,A\,cm^{-2}$ by

$$\left(\frac{\partial V}{\partial q}\right)_{i=1} = -n \ln i_0. \quad (5)$$

With $(\partial V/\partial q)_{i=1} = 1450\,V\,C^{-1}\,cm^2$, $i_0 = 3.7 \times 10^{-8}\,A\,cm^{-2}$. Data are corrected here for the roughness of the electrode surface.

A comparison of the potentiodynamic data of Fig. 6 with the galvanostatic data of Fig. 8 clearly shows that the same dependence exists between S/i_s versus $\log i$ and $\partial V/\partial q$ versus $\log i$. This suggests that the same mechanism controls the growth under both galvanostatic and potentiodynamic conditions. Differences between the respective slopes in Figs. 6 and 8, i.e. between α' in Equation 3 and $1/n$ in Equation 4, as well as between i_0 values obtained for these two modes of growth are ascribed to experimental errors particularly in the potentiodynamic experiments. Note, for instance, that the linear S/i_s versus $\log i$ relationship in the potentiodynamic experiments extends only for about 2.5 decades of i_s and the data points are somewhat scattered. In contrast, the $\partial V/\partial q$ versus $\log i$ relationship in the galvanostatic experiments extends for four decades with less scattering of the data points. Note also that the parameters V_0 and q_0 are readily obtained from the galvanostatic experiments. These parameters cannot be readily obtained from potentiodynamic experiments. Because the same mechanism controls the growth under both the galvanostatic and potentiodynamic conditions, only data from the galvanostatic experiments are used in the following analysis of the mechanism of growth.

In the simplest terms, q_0 represents the thickness of the film expressed as charge density, which is already present at the electrode surface at the time a constant current is applied to the electrode [7]. V_0 is the potential with respect to a reference electrode at which the film would begin to grow according to Equation 5 if the same law were to hold from the very early stages of film formation. V–V_0 is then the potential difference across the film, and $(V–V_0)/(q + q_0)$ represents the field within the film. Equation 4, therefore, describes the high field assisted growth of an insulating film. It should be pointed out that Equation 4 is obtained solely from experimental data without assuming any model of growth or charge distribution at the metal/anodic film/solution interface. All parameters in the equation are determined from the experimental data.

In order to assess more fully the physical significance of various parameters in the experimental rate equation, V_0, q_0, n and i_0, it is advantageous to compare them with theoretical predictions. Following Cabrera and Mott [12], the rate equation for high field growth in its simplest form and without the effect of a space charge can be written in the form [6, 12]

$$i = Nvze \exp\left(\frac{-\Delta G^*}{RT}\right) \exp\left(\frac{ze\lambda\Delta V_{of}}{kTd}\right) = i_0 \exp\left(\frac{\alpha \Delta V_{of}}{d}\right). \quad (6)$$

Here, d is the thickness of the film, ΔV_{of} is the potential difference across the film, ze is the charge of the ions migrating in the field $\Delta V_{of}/d$, and λ is the half jump distance. N is the density of the ions in the surface facing the rate determining reaction plane, and ΔG^* is the activation energy at zero field for the rate determining process. ν and k are the vibrational frequency of the migrating ions and the Boltzmann constant, respectively.

From a comparison of Equations 4 and 6, it follows that $1/n$ is equal to $ze\lambda/(rkT)$. Factor r converts charge density into thickness. With the known density of hexagonal CdS, r is calculated to be $1.55 \times 10^4\,Å\,C^{-1}\,cm^2$. Taking z as 2 for Cd^{2+} ions as the migrating species, λ determined from n is equal to 2.3 Å. Although this is on the high side, it is close to the value expected for the half jump distance. Any other value for z is either unlikely or would lead to a less reasonable half jump distance. A similar value for λ was reported

by Peter [5]. (For the present calculation of λ, RF = 1.2 was taken into account. Larger values for RF would lead to smaller values of λ, e.g. RF = 1.6 would give λ = 1.75 Å.)

The observed value for λ provides strong support for the Cabrera–Mott model of growth. It does not, however, give any indication where the rate determining step is located. This information may be obtained by an analysis of N in i_0 [6, 13]. However, before determining N, the following comments on the physical significance of d, q_0, ΔV_{of} and V_0 are called for. The significance of these parameters depends on the assumption made regarding the structure of the entire metal/anodic film/solution interface. Equation 6, strictly speaking, is valid for a simple structure with a single Helmholtz layer. The excess of positive charge in the metal is then counterbalanced by an excess of negative charge in the outermost surface of the anodic film (as surface charge) and the Helmholtz plane. For this model, ΔV_{of} is the potential difference across the anodic film, d is the thickness of the film, and $\Delta V_{of}/d$ is the field within the film. In particular, V_0 represents the potential across the solution double layer. As observed, it is a constant independent of current density. Parameter q_0 then has the significance given above. If, however, a more realistic model of the structure of the double layer is considered with the inner and outer Helmholtz layers and with the positive charge counterbalanced by an excess of negative charge in the inner and outer Helmholtz planes, but not in the outermost surface of the growing film, then the following rate equation can be derived (cf. Peter [5]):

$$i = N\nu ze \exp\left(\frac{-\Delta G^*}{RT}\right)\exp\left(\frac{ze\lambda(\phi_m - \phi_i)}{kT(d + \delta\epsilon_f/\epsilon_i)}\right). \tag{7a}$$

Here, δ is the thickness of the inner Helmholtz layer, ϕ_m is the potential at the metal, ϕ_i is the potential at the inner Helmholtz plane, ϵ_f is the dielectric constant of the anodic film, and ϵ_i is the dielectric constant of the inner Helmholtz layer. In the derivation of this equation, use was made of the known relationship between fields in two phases in contact. This relationship leads to

$$\frac{\Delta V_{of}}{d} = \frac{\phi_m - \phi_f}{d} = \frac{\phi_m - \phi_i}{d + \delta\epsilon_f/\epsilon_i} \tag{8}$$

which, with Equation 6, gives Equation 7a. ϕ_f is the potential at the outermost surface of the anodic film. Equation 8, and hence Equation 7a, are valid only if there is no excess charge at the outermost surface of the growing film. Since $\phi_m - \phi_i = V - V_0$, when V and V_0 are the potential of the electrode and the inner Helmholtz plane with respect to the same reference electrode, Equation 7a can be written in the form

$$i = i_0 \exp\left(\frac{\alpha(V - V_0)}{d + d_0}\right). \tag{7b}$$

Here, d_0 stands for $\delta\epsilon_f/\epsilon_i$. Parameter d_0, introduced with this treatment with two double layers, can be called the corrected thickness of the inner Helmholtz layer and is of atomic dimensions. Though $(V - V_0)/(d + d_0)$ still gives the field within the growing film, $V - V_0 \neq V_{of}$. V_0 is now a measure of the potential difference across the outer Helmholtz layer, and not across the entire solution double layer which was the case for the simple model. This equation can be compared with the previous equation for the simple model of the structure of the double layer, Equation 6, and the observed rate Equation 4.

The observed rate equation, on first inspection, would appear to be compatible with Equation 7b and the second model rather than with Equation 6 and the simple model with a single double layer. Parameter q_0 would then represent the corrected thickness of the inner Helmholtz layer ($d_0 = rq_0$). If so, it should be independent of electrode pretreatment and experimental conditions. The growth of sulphide films at Cd anodes resembles the growth of anodic oxide films at Pt and Ni electrodes. At Pt electrodes, q_0 was identified as the charge equivalent to the adsorbed oxygen prior to the application of a constant current and used for the formation of the oxide film in the early stages of growth. This charge varied with experimental procedure [7]. If a constant current was applied from the rest potential in N_2 saturated solutions, q_0 was smaller than when the solution was saturated with O_2. At Ni electrodes, q_0 for a particular experimental procedure used was equivalent to a thickness of 10–15 Å, far in excess of a reasonable value for the corrected thickness of the inner double layer [10]. In this case also, q_0 was defined as the charge density equivalent to the thickness of the oxide film already at the elec-

trode at the time a constant current was applied. Similarly, q_0 for the CdS formation gives a thickness of about 8 Å. Again, this value does not seem reasonable for the corrected thickness of the inner double layer. From the capacitance data, Peter [5] estimates that the corrected thickness is only about 2.4 Å. Though these examples show that q_0 in the observed rate equations represents the thickness of the anodic films prior to the application of a constant current, and is already included in d in Equations 6, 7a and 7b, the possibility that q_0 contains a contribution from the corrected thickness of the inner Helmholtz layer should not be overlooked. This contribution, if it exists, is small compared to the initial thickness, and cannot be distinguished from it with present galvanostatic experiments. Consequently, no distinction between the two models of the structure of the solution double layer and charge distribution can be made by analysing q_0. To distinguish between the models for charge distribution at the metal/anodic film/solution interface, other evidence is required. This will be discussed in a subsequent paper.

4.3. *Exchange current density*

From Equations 4 and 6, the exchange current density, i_0, is given by

$$i_0 = Nvze \exp\left(\frac{-\Delta G^*}{RT}\right). \qquad (9)$$

An analysis of ΔG^* and N can provide information regarding the rate determining step in film formation. With the data from different temperatures (Fig. 7), the activation energy, ΔG^*, can be evaluated from the slope of $\log i_0$ versus $1/T$ (Fig. 9). It is 10.6 kcal mole^{-1}. This value is low compared to activation energies in the processes of high field assisted growth of anodic oxide or hydroxide films. For the growth of $Pt(OH)_2$, for instance, ΔG^* was reported to be 25 kcal mole^{-1} in acid [14] and 18.5 kcal mole^{-1} in alkaline [13] solutions, and for the growth of $Ni(OH)_2$ in alkaline solution, 21 kcal mole^{-1} [10]. The significance of the low activation energy in CdS formation is not clear.

With $z = 2$ and taking $\nu = 10^{12}\,s^{-1}$, parameter N can now be calculated from ΔG^* and i_0. It is about $5 \times 10^6\,cm^{-2}$. This again is an unusually low value compared to N values found for the growth of anodic oxide films. For instance, at Pt, N was found to be $10^{15}\,cm^{-2}$ in acid [14] and about $10^{13}\,cm^{-2}$ in 0.1 N KOH solutions [13]. At Ni electrodes in 0.1 N KOH solutions, N was determined to be close to $10^{13}\,cm^{-2}$ [10]. So low a value for N precludes the process at the metal/sulphide film interface as the rate determining step. For such a process, N should be close to $10^{15}\,cm^{-2}$. The observed value of N is compatible with the rate determining step within the growing film with Cd^{2+} ions as the migrating species in interstitial positions. However, a process at the sulphide film/solution interface as the rate determining step cannot be ruled out. It should be noted that Equations 7a and 7b are developed for

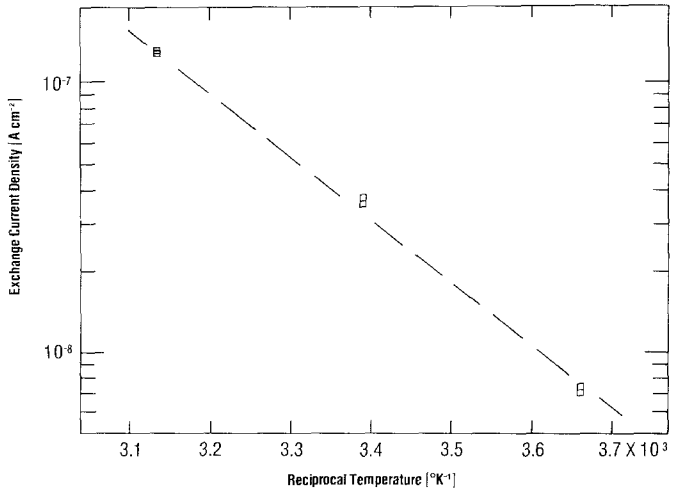

Fig. 9. Exchange current density as a function of reciprocal temperature. Data are corrected for roughness of the electrode surface (RF = 1.2).

the field within the anodic film, or at the metal/anodic film interface, affecting the processes in the rate determining step. These equations are, therefore, not directly applicable to the rate determining step at the anodic film/solution interface. Whether the process within the sulphide film or at the film/solution interface is rate determining cannot be decided from the available data. Experiments with solutions of different concentrations of Na_2S are expected to be helpful for such a determination as will be discussed in a subsequent paper.

5. Summary

In summary, the present studies show that the same kinetic equation describes the growth of thin anodic sulphide films at Cd electrodes under both galvanostatic and potentiodynamic conditions. For the growth of films up to about 50 Å, the kinetics is fully accounted for by the model of high field assisted formation of anodic films. Evidently, in this thickness range no sufficient space charge is developed to affect the kinetics. For if it were, no linear V–q or $\partial V/\partial q$–$\log i$ relationships could have been observed. The mechanism of growth remains the same over the wide range of current densities or sweep rates examined and hence of time required for film formation. It follows then that no aging of the films, or rearrangement within the films, occurs during the growth process itself. Activation energy, ΔG^*, and frequency factor, N, are substantially lower than the corresponding values for growth of anodic oxide films. The low value for N precludes a process at the Cd/CdS film interface as the rate determining step. However, neither the rate determining step nor the species participating in the step can be determined from available data. Data at different concentrations of Na_2S should be useful here. Once a critical potential and thickness are reached, the mechanism abruptly changes and films apparently of inferior quality begin to develop. What triggers these changes and causes a film of inferior quality to grow should be a subject of future research.

References

[1] B. Miller and A. Heller, *Nature* **262** (1967) 680.
[2] G. Hodes, J. Manassen and D. Cahen, *ibid.* **261** (1976) 403.
[3] L. M. Peter, *Electrochim. Acta* **23** (1978) 1073.
[4] B. Miller, S. Menezes and A. Heller, *J. Electroanal. Chem.* **94** (1978) 85.
[5] L. M. Peter, *Electrochim. Acta* **23** (1978) 165.
[6] A. Damjanovic and A. T. Ward, 'International Review of Science: Physical Chemistry', Series II, Vol. 6, Butterworths, London (1976) p. 103.
[7] A. Damjanovic and L-S. R. Yeh, *J. Electrochem. Soc.* **126** (1979) 555.
[8] M. W. Breiter and W. Vedder, *Electrochim. Acta* **13** (1968) 1405.
[9] A. Damjanovic, L-S. R. Yeh and J. F. Wolf, *J. Electrochem. Soc.* **127** (1980) 1945.
[10] J. F. Wolf, L-S. R. Yeh and A. Damjanovic, *Electrochem. Acta* **26** (1981) 811.
[11] L. B. Harris and A. Damjanovic, *J. Electrochem. Soc.* **122** (1975) 593.
[12] N. Cabrera and N. F. Mott, *Rep. Prog. Phys.* **12** (1949) 163.
[13] A. Damjanovic, L-S. R. Yen and J. F. Wolf, *J. Electrochem. Soc.* **127** (1980), 1945, 1951.
[14] *Idem, ibid.* **127** (1980) 874.